Supporting information

Full-Color Light-Emitting Carbon Dots with a Surface-State -Controlled Luminescence Mechanism

Hui Ding, *Shang-Bo Yu*, *Ji-Shi Wei* and *Huan-Ming Xiong**

Department of Chemistry, Fudan University, Shanghai 200433, P. R. China

E-mail: hmxiong@fudan.edu.cn

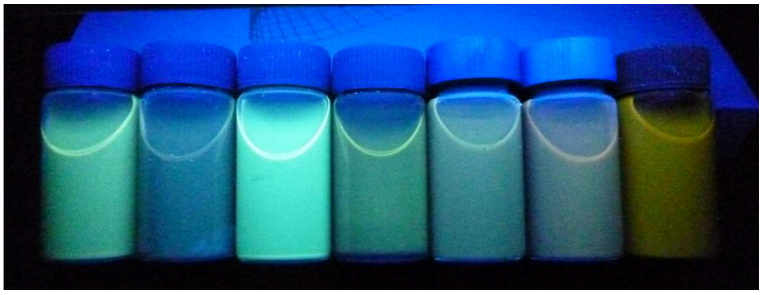

Figure S1. As-prepared reaction mixtures under irradiation with UV light. From left to right, these samples were produced by hydrothermally treating mixtures of p-phenylenediamine (0.2 g) with ethylenediamine (700 μL), 4,7,10-trioxa-1,13-tridecanediamine (700 μL), polyethyleneimine (700 μL), glucose (0.2 g), citric acid (0.2 g), L-threonine (0.2 g) and phosphoric acid (700 μL), respectively.

Figure S2. As-prepared reaction mixtures under UV light. From left to right, these samples were produced using mass ratios of urea to p-phenylenediamine of 0.1, 0.6, 1.0, 2.5, 4.0 and 6.0, respectively.

Figure S3. Reaction mixtures prepared at identical mass ratios of 1.0 (urea versus p-phenylenediamine) but different reaction temperatures under UV light. From left to right, these samples were produced at 140, 160, 180 and 200 °C, respectively.

Although the concrete formation process is far from clear, two aspects thereof are widely accepted. The first is that oxygen-containing functional groups such as -OH and -COOH are important for the formation of CDs.[1,2] The other is that the dehydrolysis reaction between carboxyl and amide is the pivotal step for the doping of N into the graphene framework.[3,4] Based on these two accepted facts and the results of the control experiments, we propose a possible formation mechanism. First, certain organic precursors acting as active molecules can be easily oxidized under hydrothermal conditions to different levels, including intermediates with carboxyl groups. Then, these precursors and intermediates undergo polymerization under subcritical conditions. During this process, the generated carboxyl groups react with the amide in urea to form pyrrolic or pyridinic N through the dehydrolysis reaction, which is the key step for linking the reagents together to form large fused rings. Finally, these polymeric fragments undergo carbonization and eventually form CDs with graphite cores and amorphous surface layers consisting of different functional groups.

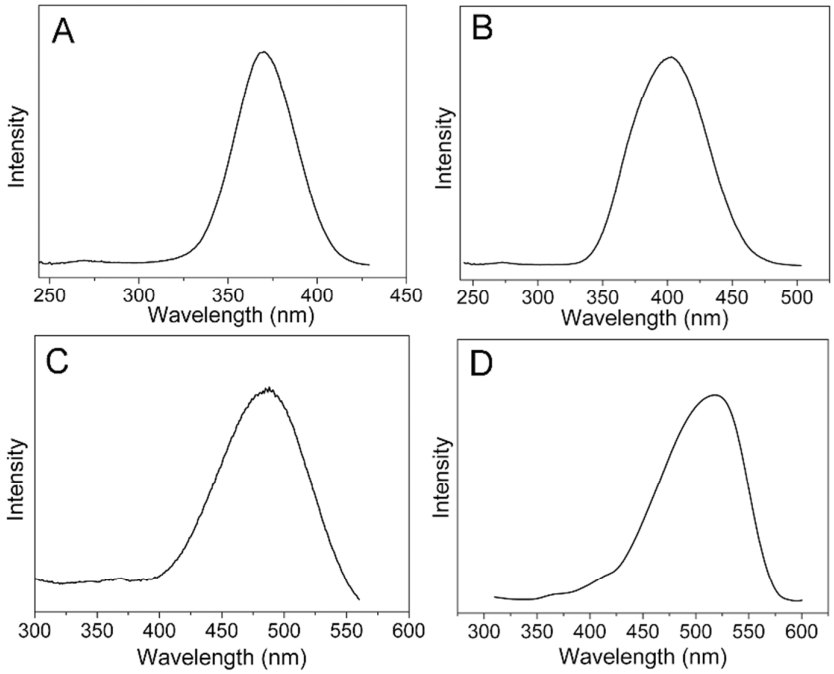

Figure S4. Excitation spectra of four typical samples obtained *via* PL detection at (A) 440, (B) 517, (C) 566 and (D) 625 nm.

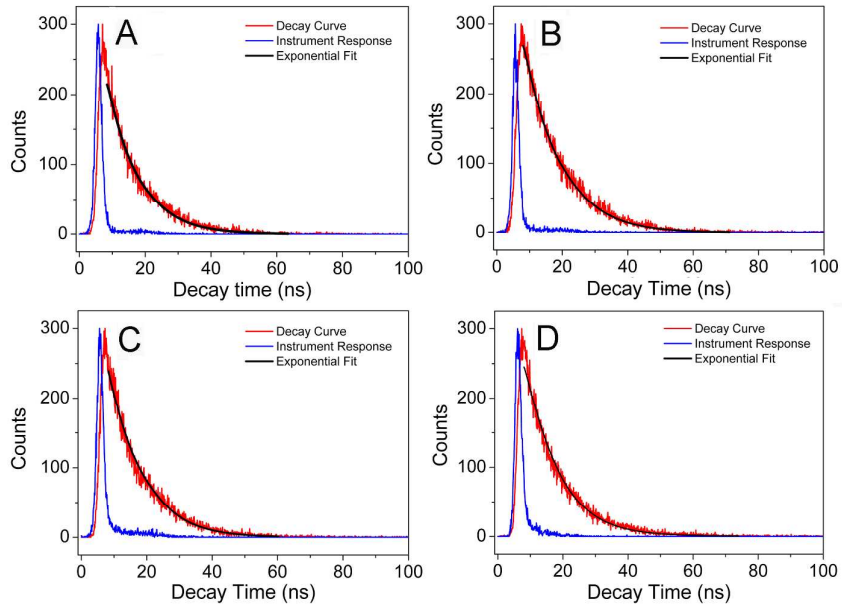

Figure S5. PL decay spectra and fitted curves for the four selected samples. These samples exhibited mono-exponential lifetimes, as shown in Table S4.

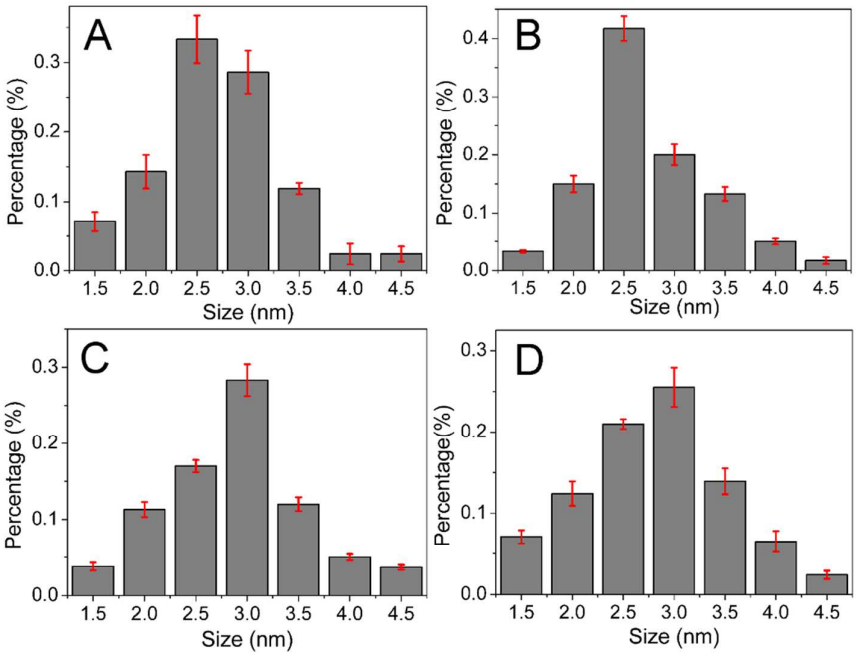

Figure S6. Histograms of the particle size distributions of the four selected samples.

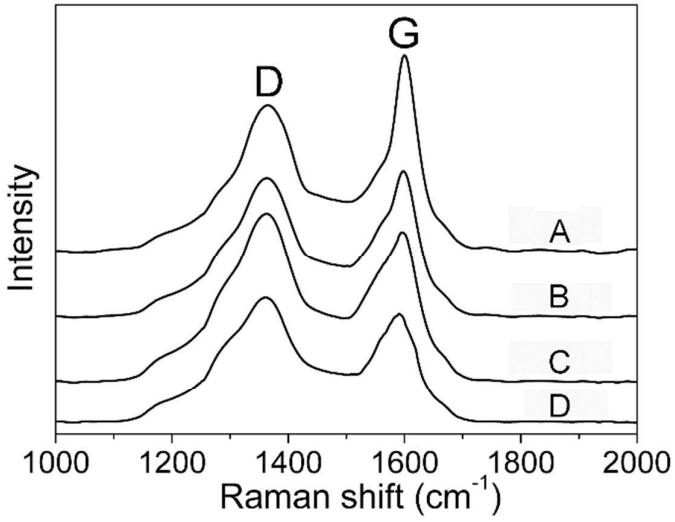

Figure S7. Raman spectra of the four selected samples.

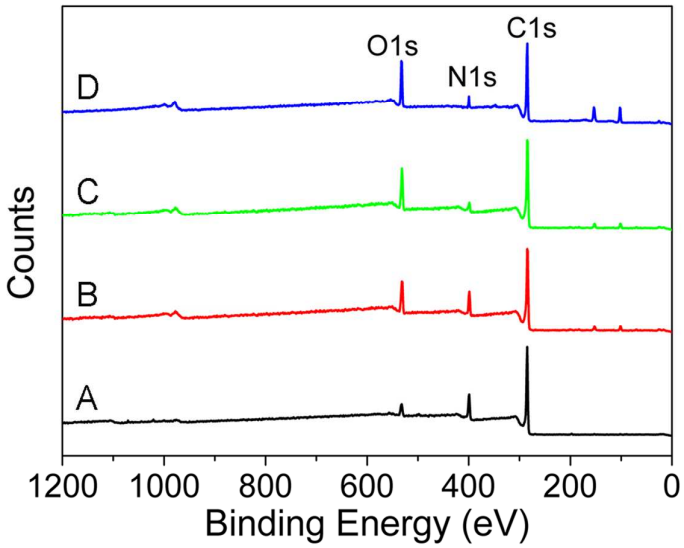

Figure S8. XPS spectra of the four selected samples.

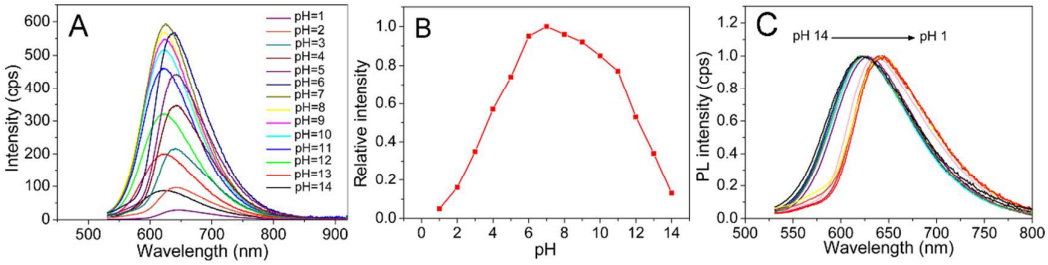

Figure S9. (A) Fluorescence spectra of the red-emitting CDs at different pH values under excitation at 520 nm. (B) Variation in the PL intensity with the pH value. (C) Normalized PL spectra for pH values varying from 14 to 1.

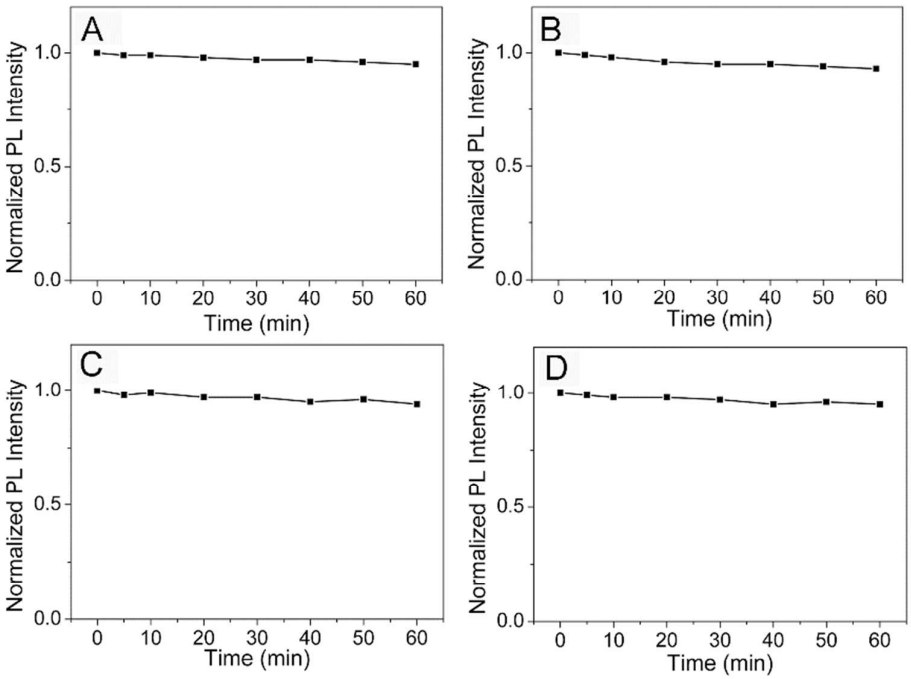

Figure S10. Photostability data for the four selected samples in water under continuous irradiation with UV light for 1 hour.

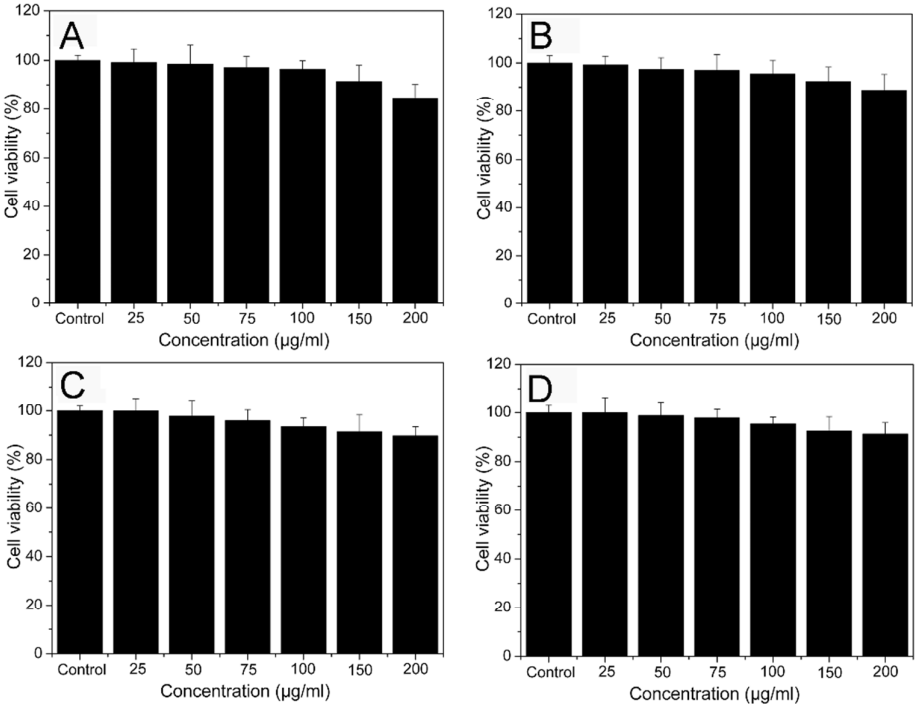

Figure S11. Cytotoxicity of the four selected samples toward HeLa cells, as assessed using the MTT method.

Table S1. Previous literature concerning CD isolation.

Ref.	Journal	Separation Method	QY (%)	PL Peak (nm)	PL Mechanism	Application
1	Angew. Chem. Int. Ed. 2007, 46, 6473	PAGE	2	415-615	Charge, Diameter	Null
2	Anal. Chem. 2012, 84, 1178	AE-HPLC	Null	408-574	Size, Charge	Null
3	J. Phys. Chem. Lett. 2013, 4, 239	HPLC	7	450-525	Charge, Surface Groups	Cell imaging
4	Talanta 2014, 129, 529	RP-HPLC	9	400-415	Size	Null
5	Electrophoresis 2014, 35, 2454	RP-HPLC	16	424-450	Size, Surface Groups	Null
6	Nanoscale 2014, 6, 8162	RP-HPLC	9	446-490	Surface Groups, Graphitization	Cell imaging
7	J. Chromatogr. A 2013, 1304, 234	CE	43	Null	Charge, Surface Groups	Null

Table S2. PL scan conditions and QY data for the as-prepared CDs.

Sample	Excitation (nm)	Emission (nm)	PL range 1 (nm)	PL range 2 (nm)	Quantum yield (%)
1	371	440	361-381	386-722	21.23
2	378	458	368-388	393-736	13.18
3	404	517	394-414	419-788	8.53
4	467	553	457-477	482-900	19.64
5	482	566	472-492	497-900	27.57
6	493	582	483-503	508-900	35.14
7	511	594	501-521	526-900	29.62
8	521	625	511-531	536-900	23.81

Table S3. QY data for the as-prepared CDs excited by 365 nm UV light.

Sample	1	2	3	4	5	6	7	8
QY (%)	20.51	11.75	6.18	12.69	18.83	24.50	20.33	14.19

Table S4. TRPL results for the four selected samples in water.

Sample	λ_{ex} [nm]	λ_{em} [nm]	τ [ns]	Percentage [%]	χ^2
A	371	440	8.94	100	1.17
B	404	517	10.05	100	1.01
C	482	566	9.30	100	1.16
D	521	625	9.41	100	1.11

Table S5. Elemental compositions of the four selected samples as determined *via* XPS.

Sample	C (%)	N (%)	O (%)
A	78.30	15.70	6.00
B	77.73	11.19	11.07
C	76.40	5.40	18.20
D	73.09	6.71	20.20

Table S6. XPS data analyses of the O1s spectra of the four selected CD samples.

Sample	C=O (%)	C-O (%)
A	20.42	79.58
B	43.80	56.20
C	52.30	47.70
D	75.49	24.51

References:

(1) Zhu, S.; Meng, Q.; Wang, L.; Zhang, J.; Song, Y.; Jin, H.; Zhang, K.; Sun, H.; Wang, H.; Yang, B. Highly Photoluminescent Carbon Dots for Multicolor

Patterning, Sensors, and Bioimaging. *Angew. Chem., Int. Ed.* **2013**, *52*, 3953-3957.

(2) Hu, L.; Sun, Y.; Li, S.; Wang, X.; Hu, K.; Wang, L.; Liang, X.-j.; Wu, Y. Multifunctional Carbon Dots with High Quantum Yield for Imaging and Gene Delivery. *Carbon* **2014**, *67*, 508-513.

(3) Qu, D.; Zheng, M.; Zhang, L.; Zhao, H.; Xie, Z.; Jing, X.; Haddad, R. E.; Fan, H.; Sun, Z. Formation Mechanism and Optimization of Highly Luminescent N-Doped Graphene Quantum Dots. *Sci. Rep.* **2014**, *4*, 5294.

(4) Song, Y.; Zhu, S.; Zhang, S.; Fu, Y.; Wang, L.; Zhao, X.; Yang, B. Investigation from Chemical Structure to Photoluminescent Mechanism: a Type of Carbon Dots from the Pyrolysis of Citric Acid and an Amine. *J. Mater. Chem. C* **2015**, *3*, 5976-5984.